SCIENTIFIC REPORTS

A serum ''sweet-doughnut'' protein facilitates fibrosis evaluation and therapy assessment in patients with viral hepatitis

Atsushi Kuno[1]*, Yuzuru Ikehara[1]*, Yasuhito Tanaka[2], Kiyoaki Ito[3], Atsushi Matsuda[1], Satoru Sekiya[1], Shuhei Hige[4], Michiie Sakamoto[5], Masayoshi Kage[6], Masashi Mizokami[3] & Hisashi Narimatsu[1]

[1]Research Center for Medical Glycoscience (RCMG), National Institute of Advanced Industrial Science and Technology (AIST), Tsukuba, Japan, [2]Department of Virology & Liver Unit, Nagoya City University Graduate School of Medical Sciences, Nagoya, Japan, [3]The Research Center for Hepatitis and Immunology, National Center for Global Health and Medicine, Ichikawa, Japan, [4]Department of Internal Medicine, Hokkaido University Graduate School of Medicine, Sapporo, Japan, [5]Department of Pathology, School of Medicine, Keio University, Tokyo, Japan, [6]Department of Pathology, Kurume University School of Medicine, Kurume, Japan.

Although liver fibrosis reflects disease severity in chronic hepatitis patients, there has been no simple and accurate system to evaluate the therapeutic effect based on fibrosis. We developed a glycan-based immunoassay, FastLec-Hepa, to fill this unmet need. FastLec-Hepa automatically detects unique fibrosis-related glyco-alteration in serum hyperglycosylated Mac-2 binding protein within 20 min. The serum FastLec-Hepa counts increased with advancing fibrosis and illustrated significant differences in medians between all fibrosis stages. FastLec-Hepa is sufficiently sensitive and quantitative to evaluate the effects of PEG-interferon-α/ribavirin therapy in a short post-therapeutic interval. The obtained fibrosis progression is equivalent to -0.30 stages/year in patients with sustained virological response, and 0.01 stages/year in relapse/nonresponders. Furthermore, long-term follow-up of the severely affected patients found hepatocellular carcinoma developed in patients after therapy whose FastLec-Hepa counts remained above a designated cutoff value. FastLec-Hepa is the only assay currently available for clinically beneficial therapy evaluation through quantitation of disease severity.

T
he World Health Organization has estimated that the prevalence of chronic infections with hepatitis B virus (HBV) and hepatitis C virus (HCV) is more than 5% of the world population. The high rate of viral transmission worldwide has also resulted in an explosive increase in incidence of liver cirrhosis (LC), because liver fibrosis caused by the persistent infections with HBV and HCV irreversibly progresses in chronic hepatitis (CH) patients without effective treatment. As the incidence of hepatocellular carcinoma (HCC) increases proportionally to the severity of hepatitis and the presence of LC, it is now clear that about 90% of HCC cases originate from infection with HBV or HCV. It is estimated that more than one million patients worldwide die from liver disease related to HBV or HCV infection each year. Immunomodulatory therapy with PEG-interferon-α and ribavirin is the standard treatment for patients with chronic hepatitis C (CHC)[1]. Recent genome-wide association studies have revealed that variation in the host interleukin-28B gene can predict the outcome of therapies for viral clearance[2–4]. Such pharmacokinetic understanding should allow for more precise treatment protocols and follow-up analyses to optimize the opportunity for patients to achieve sustained viro-logical response (SVR)[5,6]. Linear peptidomimetic HCV and NS3/4A serine protease inhibitors such as telaprevir and boceprevir are new drugs that, in combination with PEG-interferon-α and ribavirin, substantially improve the rates of response among patients with HCV genotype 1 infection[1]. Alternatively, suppression of hepatic decompensation in chronic hepatitis B patients with advanced fibrosis and cirrhosis has been evaluated during long-term treatment with antiviral agents, such as adefovir, lamivudine, entecavir, and tenofovir[7]. For example, cumulative entecavir therapy (for at least 3 years) resulted in substantial histological improvement and regression of fibrosis or cirrhosis[8].

The efficacy of therapy is currently evaluated by frequent monitoring of "viral load" or "liver injury"[5]. From the viewpoint of developing preventive strategies for HCC, the risk of HCC development should also be estimated along with them. For this purpose, liver biopsy is generally considered as the gold standard in which fibrosis is subclassified into 5 stages of severity (F0–4). However, this procedure is invasive and shown to cause a high rate of sampling error (about 15% false-negatives for cirrhosis) in patients with diffuse parenchymal liver diseases.

Furthermore, in a retrospective cohort study[9], the rate of fibrosis progression was estimated at about −0.28 stages/year in patients with SVR and 0.02 stages/year in patients with nonsustained virological response (NVR). This indicates that the biopsy is not suitable for evaluating the effect of therapy after a short interval. The procedure has further disadvantages such as inaccuracy, biopsy-related complications, the need for hospitalization, the time involved, and low cost-effectiveness[10]. Therefore, alternative noninvasive assays are desired and should provide a quantifiable readout of fibrosis progression using a method that is accurate, cost-effective and relatively simple.

To date, several methods have been developed[10] including FibroScan, which measures hepatic fibrosis biomechanically as tissue stiffness based on transient elastography. FibroScan has the advantages of being rapid and technically simple; however, its diagnostic success rate is affected by operator skill. Therefore, it has been suggested that FibroScan, in conjunction with assay of serum fibrosis biomarkers, should improve diagnostic accuracy. FibroTest[11] and FibroMeter[12], believed to be the most reliable indices of fibrosis, have been used in the combination assay aiming to eliminate the need for liver biopsy[13,14]. However, FibroTest and FibroMeter do not complement FibroScan in the development of a rapid "on-site diagnosis" system. This is because each requires both extensive and specialized blood analyses (FibroTest requires α2-macroglobulin, apolipoprotein A1, haptoglobin, γ-glutamyltransferase and total bilirubin whereas FibroMeter requires platelet count, prothrombin index, AST, α2-macroglobulin, hyaluronic acid and urea). In addition, both tests require data on age, and also sex for FibroTest.

Glycans are referred to as the face of cells, which reflect their status such as differentiation stage rather than their state of damage, and therefore they can be great markers for chronic disease. In the case of hepatitis, glycans are considered to reflect more specifically the progression of fibrosis than viral load. In the search for a simple and rapid method that is not markedly affected by tissue inflammation and ALT fluctuation, the possibility of glycomic and glycoproteomic techniques has emerged[15,16], and there are reports of some successful examples applicable for use in the clinical laboratories[17–19]. However, the current glycomic techniques require at least 3 hours of sample preparation for analysis and this has markedly reduced the combination use of glycan-based immunoassays with FibroScan. In this report, we describe for the first time, a rapid and simple glycan-based immunoassay, FastLec-Hepa, that can quantify fibrosis as precisely as FibroTest and also readily evaluate the antifibrotic effects of therapy at the clinical site (**Supplementary Fig. 1**). Moreover, we introduce a novel method for rational selection of the "non-fucose binding type" lectins and provide details of how this concept can be adopted for future development of clinically useful glyco-diagnostic tools.

Results

Changes in the N-glycosylation of M2BP during progression of liver disease. Based on previous reports[20–23], we adopted the serum 90 K/Mac-2 binding protein (M2BP) as a glycoprotein biomarker for liver fibrosis. M2BP is secreted from many cell types, including hepatocytes (http://www.proteinatlas.org/ENSG00000108679), and it has been shown to modulate many processes, particularly those related to cell adhesion. For example, the interaction of M2BP with matrix fibronectin can modulate adhesion and the high expression of M2BP by tumor cells increases the level in the circulation of affected patients. A prominent feature of native human M2BP is its oligomerization to large ring structures[20], resembling a "sugar-powdered doughnut" which is potentially covered with 70–112 N-glycans (**Fig. 1a**). To confirm serum M2BP as a valid marker, we performed a pull-down assay with serum (2 μl each) from five individuals in each of the following groups: HCC, LC, CHC or healthy volunteer with normal liver (HV). Although two bands

appeared in all HVs and two CHC patients, M2BPs from patients with relatively severe fibrosis, i.e., LC and HCC, migrated as a single band, the mobility of which was similar to that of the lower band for HVs (**Fig. 1b**). Significant increases in band intensity with excessive smearing of the bands were seen for most HCC patients. A subsequent investigation of 125 HCV patients with stage-determined fibrosis showed alteration in the quality and quantity of M2BP during the progression of fibrosis (**Fig. 1c**) and apparent alteration in the amount of each band (**Fig. 1d and e**), as described in the previous investigations[22,23]. M2BP has been shown to have multibranching and sialylated N-glycans. Moreover, it has been suggested that extension of polylactosamine on M2BP controls its binding to galectin-3, a major binding partner in vivo. Sialylation and extension of polylactosamine affect the charge and size of M2BP and this results in altered electrophoretic migration. Accordingly, we speculate that the size heterogeneity of M2BP seen on electrophoresis is due to such alterations in glycosylation. In fact, the difference in the band migration was eliminated by Sialidase A treatment, and the smearing of the bands in HCC was reduced by treatment with N-Glycosidase F (**Supplementary Fig. 2**). These results indicated that the altered quality of M2BP during progression of liver disease was due to changes in N-glycosylation.

Selection of the optimal lectin for direct measurement of disease-related M2BP. To construct a reliable assay (see **Supplementary Fig. 3**), we needed to identify a lectin probe that could most readily discriminate the altered N-glycans of M2BP and specifically binds to them in serum without pretreatment. For this purpose, we added a subtraction process to our recently described microarray-based selection strategy[16] (**Supplementary Fig. 4**). In brief, we first obtained a typical glycan profile for serum M2BPs by averaging the glycan profiles of M2BPs immunoprecipitated from 125 HCV patient sera by the antibody-overlay lectin microarray[16,18,24] (**step 1**). In this step, we selected 27 lectins binding to M2BP from a 45-lectin array (**Supplementary Fig. 5a**). Most of them bound not only to M2BP (ca. 10 μg/ml in serum), but also to other abundant serum glycoproteins, whereas some suggested rather specific binding to M2BP. We designated them as high-noise lectins or high signal-to-noise (S/N) lectins, respectively (**Fig. 2a**). We then selected the candidate lectins for the assay by subtracting the high-noise lectins from the M2BP-binding lectins (**step 2**), using a glycan profile of whole serum (**Supplementary Fig. 5**)[25]. Comparing the profiles for M2BP and whole serum (**Fig. 2b**), we quickly identified 6 lectins with a high S/N ratio. Interestingly, all lectins identifying fucose modification, which is the most well-known glyco-alteration in liver disease (Pisum sativum agglutinin (PSA), Lens culinaris agglutinin (LCA), Aspergillus oryzae lectin (AOL), and Aleuria aurantia lectin (AAL)), were high-noise lectins (**Fig. 2b**). After subtraction, we used both the Mann–Whitney U test as a nonparametric test, and receiver-operating characteristic (ROC) analysis, to characterize the diagnostic accuracy of the candidate lectins at each stage of fibrosis: significant fibrosis (F2/F3/F4), severe fibrosis (F3/F4) and cirrhosis (F4) (**step 3**). As a result, we found that the diagnostic score of Wisteria floribunda agglutinin (WFA) was superior to the other 5 lectins at every fibrosis stage (**Fig. 2c and Supplementary Fig. 6**).

"Proof-of-concept" experiment for direct quantitation of the serum WFA-binding M2BP by sandwich immunoassay. We quantitatively analyzed the WFA-binding M2BPs (WFA⁺-M2BP) in serum. Sera, pretreated as described in the **Methods**, were firstly subjected to affinity capture with 20 μl slurry of WFA-coated agarose gel. The eluted fraction was immunoprecipitated with a capturing antibody against M2BP and the product was analyzed by Western blot. The intensity of the "smearing-band" signal for WFA⁺-M2BP gradually increased in proportion to the severity of liver fibrosis (**Supplementary Fig. 7**), as indicated by the red line shown in
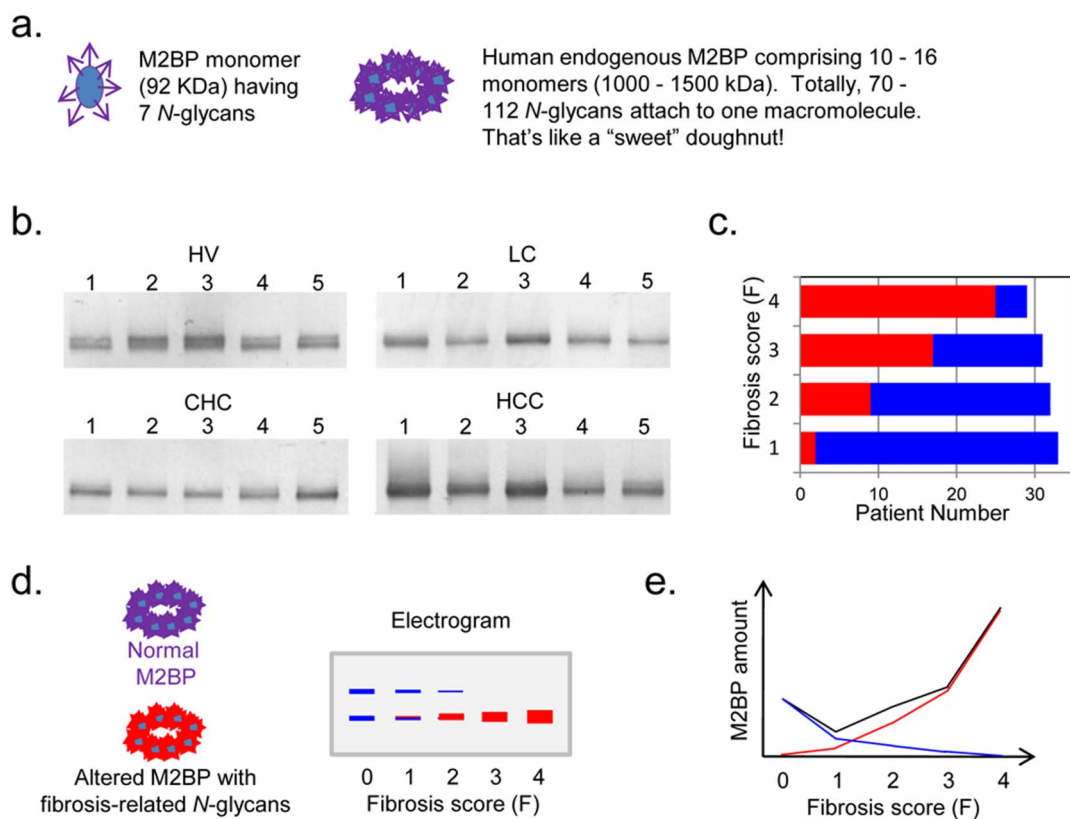
Figure 1 | Changes in the quality and quantity of human serum M2BP with progression of liver fibrosis. (a) The unique shape of human endogenous serum M2BP. The arrowheads and circles represent the *N*-glycan moieties and core protein respectively. (b) Western blot analysis: M2BPs in 2 μl of serum were purified by immunoprecipitation before SDS-PAGE. HV, healthy volunteer; CHC, patient with chronic hepatitis C; LC, HCV-infected patient with liver cirrhosis; and HCC, HCV-infected patient with hepatocellular carcinoma. (c) Number of patients with single (red) or double (blue) band appearance on the blot. The number of bands was determined visually by two independent analysts. The total number of HCV patients who participated in this study was 125 (F0–F1 [*n* = 33], F2 [*n* = 32], F3 [*n* = 31], and F4 [*n* = 29]). (d) Typical changes of serum M2BP band intensities in patients with different fibrosis scores and (e) concentrations based on a previous report on quantitation of serum M2BP by Cheung *et al*[3]. and our present results. The blue bands on the electrogram and blue line on the graph represent M2BPs secreted from normal liver. The red bands and line represent altered M2BP, the concentration of which is suggested to increase with the progression of fibrosis. The black line represents the total concentration of serum M2BP.

Fig. 1e. We next conducted a sandwich immunoassay with WFA and anti-M2BP antibody (see **Supplementary Fig. 3b**). WFA was immobilized on the surface of a 96-well microtiter plate through biotin–streptavidin interaction. We performed the first assay for the WFA-binding activity using recombinant human M2BP (rhM2BP). As a result, a linear regression analysis revealed a linear range of detection from 0.039 to 0.625 μg/ml (**Supplementary Fig. 8a**). Subsequently, we used culture supernatant of a hepatoblastoma cell line HepG2, which expresses WFA⁺-M2BP, to illustrate the dose-dependency of the interaction of WFA with M2BP/HepG2. We also showed that heat treatment of the culture supernatant eliminated this binding activity (**Supplementary Fig. 8b**). Finally, we performed a sandwich immunoassay for direct measurement of WFA⁺-M2BP in untreated serum samples, and the results correlated well with the quantitative assay using affinity capture and lectin microarray analysis (**Supplementary Fig. 7 and 9**).

FastLec-Hepa: a fully automated sandwich immunoassay for direct quantitation of serum WFA⁺-M2BP. We adapted the WFA-antibody immunoassay to the HISCL-2000i bedside clinical chemistry analyzer[18]. We successfully adjusted every reaction condition during the automatic assay by HISCL, which is about a 17-min manipulation. Heat pretreatment of the serum was avoided to ensure both binding avidity and the fast association rate. Repeatability was assessed by performing 10 independent assays of three samples, and the coefficient of variation ranged between 2.1%

and 2.5% (data not shown). Sensitivity was determined by triplicate assays of samples generated by 2-fold serial dilution of 50 μg/ml rhM2BP. The linear regression analysis identified a linear range of detection ($R^2 = 1.00$) from 0.025 to 12.5 μg/ml (**Fig. 3a**, a range of 0.025 to 1.6 μg/ml also shown in **Fig. 3b**). The resulting dynamic range was 25-fold that of the manual sandwich immunoassay described above. We next examined whether the HISCL measurements made on serum from HCV patients (*n* = 125) were consistent with lectin microarray analysis, and this comparison resulted in sufficient linearity with coefficient of determination, $R^2 = 0.848$ (**Fig. 3c**). Accordingly, we could perform automatic quantitation of serum WFA⁺-M2BP in 180 patients in 1 hour and we have therefore named it FastLec-Hepa.

Validation of FastLec-Hepa. For a validation study, we obtained serum from CH patients at two locations: Nagoya City University Hospital and Hokkaido University Hospital (**Supplementary Fig. 10**). Staging of these patients (*n* = 209) by histological activity index (HAI) was conducted independently by two senior pathologists on ultrasonography-guided liver biopsy samples. F0–F1 was assigned in 82 cases (39.2%), F2 in 52 (24.9%), F3 in 40 (19.1%), and F4 (cirrhosis) in 35 (16.7%). Serum from healthy volunteers (with no history of any hepatitis virus infections) was obtained for analysis from two sites (*n* = 48 from National Institute of Advanced Industrial Science and Technology [AIST]: HV1; *n* = 70 from Nagoya City University: HV2). Their FastLec-Hepa counts
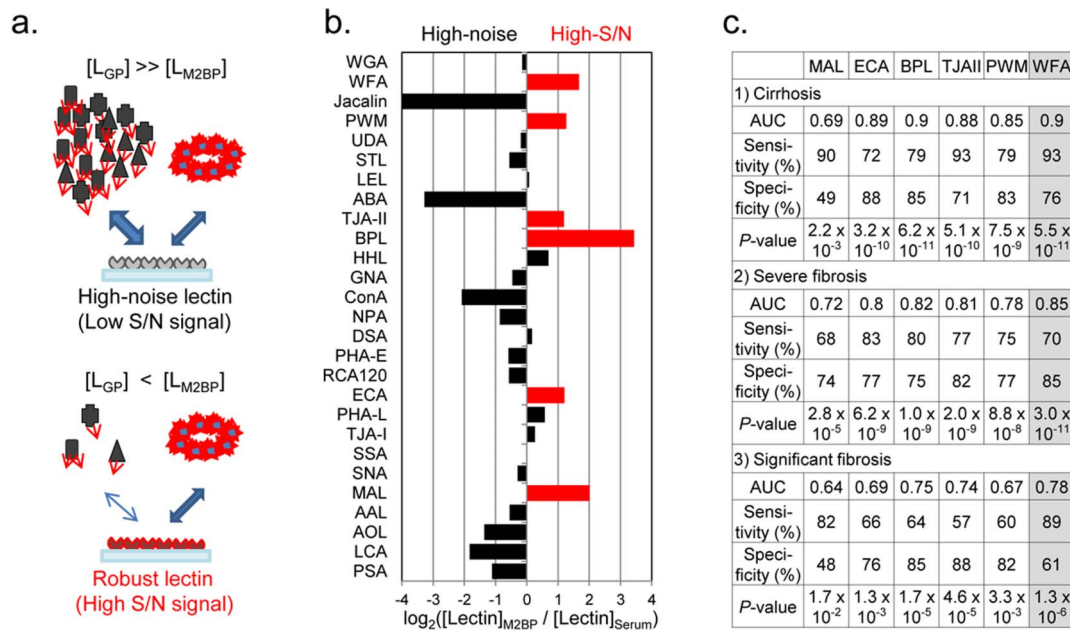
3

Figure 2 | Selection of the optimal lectin for the lectin-antibody sandwich immunoassay. (a) The kinetics of lectins binding to serum glycoproteins. The M2BP-binding lectins are divided into two categories: high-noise lectins and high signal-to-noise (S/N) lectins. The high-noise lectins bind to both M2BPs and abundant serum glycoproteins, causing a strong suppression of the M2BP–lectin interaction (see *top panel*). On the other hand, the number of binding targets in serum for the high S/N lectins is negligible, resulting in the specific interaction with the target M2BP (see *lower panel*). (b) Classification of M2BP-binding lectins. The high S/N lectins are those detecting M2BPs with at least twice the signal intensity seen for other serum glycoproteins. The classification strategy is summarized in **Supplementary Fig. 4**. (c) Diagnostic performance of 6 candidate lectins. *P*-values were determined using the nonparametric Mann–Whitney *U* test (Excel 2007, Microsoft).

	MAL	ECA	BPL	TJAII	PWM	WFA
1) Cirrhosis						
AUC	0.69	0.89	0.9	0.88	0.85	0.9
Sensitivity (%)	90	72	79	93	79	93
Specificity (%)	49	88	85	71	83	76
P-value	2.2×10^{-3}	3.2×10^{-10}	6.2×10^{-11}	5.1×10^{-10}	7.5×10^{-9}	5.5×10^{-11}
2) Severe fibrosis						
AUC	0.72	0.8	0.82	0.81	0.78	0.85
Sensitivity (%)	68	83	80	77	75	70
Specificity (%)	74	77	75	82	77	85
P-value	2.8×10^{-5}	6.2×10^{-9}	1.0×10^{-9}	2.0×10^{-9}	8.8×10^{-8}	3.0×10^{-11}
3) Significant fibrosis						
AUC	0.64	0.69	0.75	0.74	0.67	0.78
Sensitivity (%)	82	66	64	57	60	89
Specificity (%)	48	76	85	88	82	61
P-value	1.7×10^{-2}	1.3×10^{-3}	1.7×10^{-5}	4.6×10^{-5}	3.3×10^{-3}	1.3×10^{-6}

(**Supplementary Table 1**) are also plotted in a box-whisker diagram in **Supplementary Fig. 11** along with that from a separate group of 1,000 healthy volunteers (HV3). Based on the calibration curve ([FastLec-Hepa counts]$/10^6 = 1.027 \times$ [rhM2BP] + 0.006 in **Fig. 3a, b**), the 75th percentiles of HVs of 64,205–107,617 and the 25th percentile of LC of 1,327,596 patients (see also **Supplementary Fig. 11**), we estimate the concentration of WFA$^+$-M2BP to be approximately 0.09 μg/ml in the serum of HV patients and > 1.0 μg/ml in that of LC patients. This means that the linear range shown in **Fig. 3a** is sufficient for accurate quantitation of WFA$^+$-M2BP in all serum samples. The analyses showed a gradual increase with the progression of liver fibrosis, but it did not correlate with the grade of hepatic activity defined by HAI scoring (**Supplementary Fig. 12**).

Next, we made a statistical comparison of FastLec-Hepa with other simple tests for liver fibrosis: the direct fibrosis marker hyaluronic acid (HA), the indirect fibrosis index FIB-4[26] and the glycan-based fibrosis index LecT-Hepa[18,27]. We enrolled 160 patients (F0−F1 = 66, F2 = 41, F3 = 33 and F4 = 20) whose age, platelet count, AST, ALT and HA levels were readily available (**Supplementary Fig. 10** and **Supplementary Tables 1 and 2**). As shown in **Fig. 4a**, the results of all the tests correlated well with the stage of fibrosis ($P < 0.0001$). However, an ROC analysis concluded that FastLec-Hepa detected cirrhosis with the highest diagnostic accuracy (**Fig. 4b** and **Table 1**). Notably, FastLec-Hepa distinguished between F3 and F4 with 90% sensitivity, 85% specificity, and with an AUC of 0.91. These results were superior to LecT-Hepa (sensitivity:
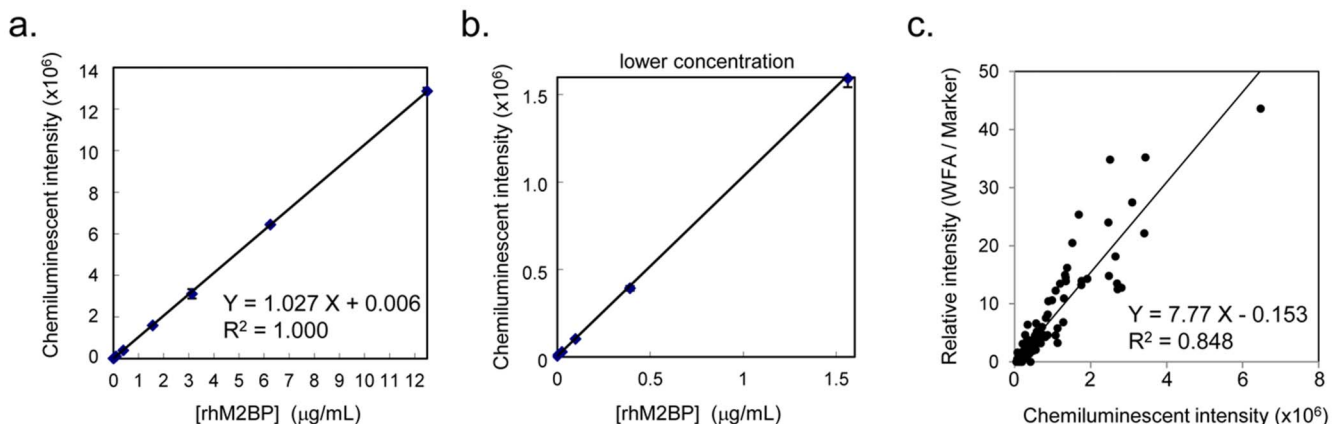

Figure 3 | Description of FastLec-Hepa, a fully automated WFA and anti-M2BP antibody sandwich immunoassay. (a) Standard curve for quantitation of WFA-binding rhM2BP. Plots for the lower concentration of rhM2BP are alternatively highlighted in (b). (c) Scatterplot comparison of WFA$^+$-M2BP data obtained from 125 different serum samples by both HISCL and a manual lectin microarray assay. The best-fit linear comparison with its correlation coefficient was calculated in Excel 2007 (Microsoft).
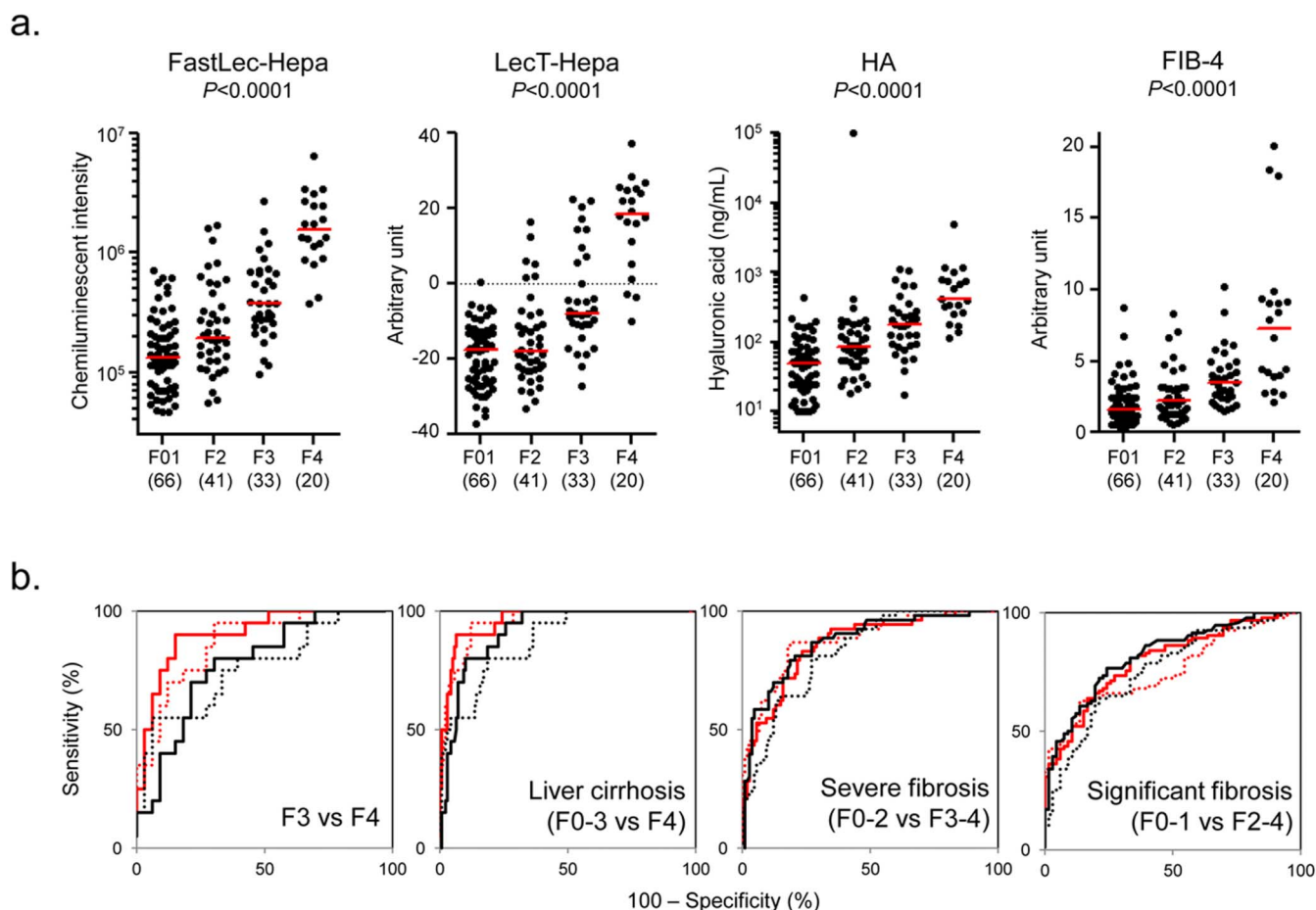
Figure 4 | Comparison of diagnostic performance of FastLec-Hepa, LecT-Hepa, HA, and FIB-4. (a) Scatterplots of the data obtained with FastLec-Hepa, LecT-Hepa, HA, and FIB-4 against the fibrosis score. Red horizontal lines represent the median. Correlation of the data with the progression of fibrosis was evaluated as significant differences in the medians relative to the fibrosis scores ($P < 0.0001$) by a nonparametric method, the Kruskal–Wallis one-way ANOVA. (b) Area under the receiver-operating characteristic (AUC-ROCs) curves of FastLec-Hepa, LecT-Hepa, HA, and FIB-4 for liver cirrhosis (F3 vs F4 or F0–3 vs F4), severe fibrosis (F0–2 vs F3–4), and significant fibrosis (F0–1 vs F2–4). FastLec-Hepa, LecT-Hepa, HA, and FIB-4 are indicated by a red solid line, red dotted line, black solid line, and black dotted line, respectively.

95%, specificity: 70%, and AUC: 0.87), FIB-4 (sensitivity: 55%, specificity: 94%, and AUC: 0.76), and HA (sensitivity: 80%, specificity: 70%, and AUC: 0.78).

Clinical utility of FastLec-Hepa: quantitative monitoring of antiviral therapy. To assess clinical utility, we examined two types of trials—short-interval evaluation and long-term follow-up—both of which are essential for following the patients receiving PEG-interferon-α and ribavirin therapy. For the first trial, we enrolled 41 patients with CHC who had previously undergone 48 weeks of therapy at Hokkaido University Hospital. According to the definition described in the **Methods**, 26 and 15 of them were judged as SVR and NVR/relapse (non-SVR), respectively. For each patient, we performed FastLec-Hepa on serum samples, which were collected just before treatment (Pre) and within a short period (12–22 weeks) after treatment (Post) (**Fig. 5a**). We found a marked decrease from Pre to Post counts ($P = 0.0061$) in SVR patients, but no apparent change for non-SVR patients ($P = 0.9780$) (**Fig. 5b**). Specifically, a median percent decrease of 31% was found for SVR patients (median Pre-count of 161,053 and median Post-count of 110,739), while the level for non-SVR patients was essentially constant. These results show that the assay can evaluate the effect of therapy within a short period after treatment. This is an important advance, because the ALT levels of non-SVR, as well as SVR, are mostly decreased into the range of 10–64 IU/ml during this

period (**Fig. 5c**)[5]. In fact, changes in the FastLec-Hepa counts did not correlate with those in the ALT counts (**Supplementary Fig. 13**), thereby invalidating ALT-dependent fibrosis assays, including FIB-4 (**Fig. 5d**).

In support of our finding that the FastLec-Hepa counts correlate excellently with the stage of fibrosis, we found a strong correlation between the histopathological scores and the median of the $\log_{10}$[FastLec-Hepa] counts (**Fig. 5e**). These correlations were approximated to two linear equations: $y = 0.23x + 4.9$ for F0 to F3, and $y = 0.58x + 3.8$ for F3 to F4 histology. This means that FastLec-Hepa can reliably reproduce the assessment of therapeutic effects, which were previously drawn from histopathological scoring[9]. Indeed, the median changes in fibrosis obtained by FastLec-Hepa analysis were about −0.295 stages/year for SVR and 0.010 stages/year for non-SVR (**Fig. 5f**). These data were consistent with the rate of fibrosis progression and regression determined by Shiratori et al[9].

For the second trial, we enrolled 6 HCV patients (SVR = 3 and non-SVR = 3) with advanced fibrosis who completed 48 weeks of therapy at Nagoya City University Hospital. Sera were collected before therapy and at 0, 1, 3, and 5 years after the end of therapy (see **Fig. 5g**). FastLec-Hepa counts in SVR patients gradually decreased and reached below the median of F0 patients within 3 years. However, those in non-SVR patients remained above the median for F3 patients during the follow-up period (**Fig. 5h**).

Table 1 | Diagnostic performance of fibrosis markers

n = 160	FIB-4	HA	LecT-Hepa	FastLec-Hepa
a) Significant fibrosis (F0–1 vs F2–4)				
AUC	0.76	0.82	0.76	0.79
(95% CI)	(0.68–0.83)	(0.76–0.89)	(0.69–0.83)	(0.72–0.86)
Diagnostic sensitivity (%)	64	77	63	81
Diagnostic specificity (%)	79	76	86	67
Youden's index (%)	43	52	49	48
b) Severe fibrosis (F0–2 vs F3–4)				
AUC	0.83	0.87	0.88	0.84
(95% CI)	(0.76–0.89)	(0.81–0.93)	(0.82–0.93)	(0.77–0.91)
Diagnostic sensitivity (%)	81	81	87	83
Diagnostic specificity (%)	71	79	81	77
Youden's index (%)	52	61	68	60
c) Liver cirrhosis (F0–3 vs F4)				
AUC	0.88	0.91	0.95	0.96
(95% CI)	(0.80–0.95)	(0.86–0.96)	(0.92–0.99)	(0.93–0.99)
Diagnostic sensitivity (%)	80	80	95	90
Diagnostic specificity (%)	81	90	88	94
Youden's index (%)	61	70	83	84
d) Liver cirrhosis (F3 vs F4)				
AUC	0.76	0.78	0.87	0.91
(95% CI)	(0.63–0.90)	(0.65–0.90)	(0.77–0.97)	(0.82–0.99)
Diagnostic sensitivity (%)	55	80	95	90
Diagnostic specificity (%)	94	70	70	85
Youden's index (%)	49	50	65	75

Interestingly, HCC had developed in two non-SVR patients whose FastLec-Hepa counts remained above the median of F4 patients throughout. Other fibrosis indices, such as FIB-4 and biochemical parameters (ALT and AST), did not distinguish between SVR and non-SVR or appear to predict this occurrence (**Fig. 5i-k**).

Discussion

We have described the development and use of a fully automated, glycan-based immunoassay termed FastLec-Hepa, for the evaluation of liver fibrosis. A high degree of reliability in the quantitative aspects of this method should establish it as a clinically significant test,
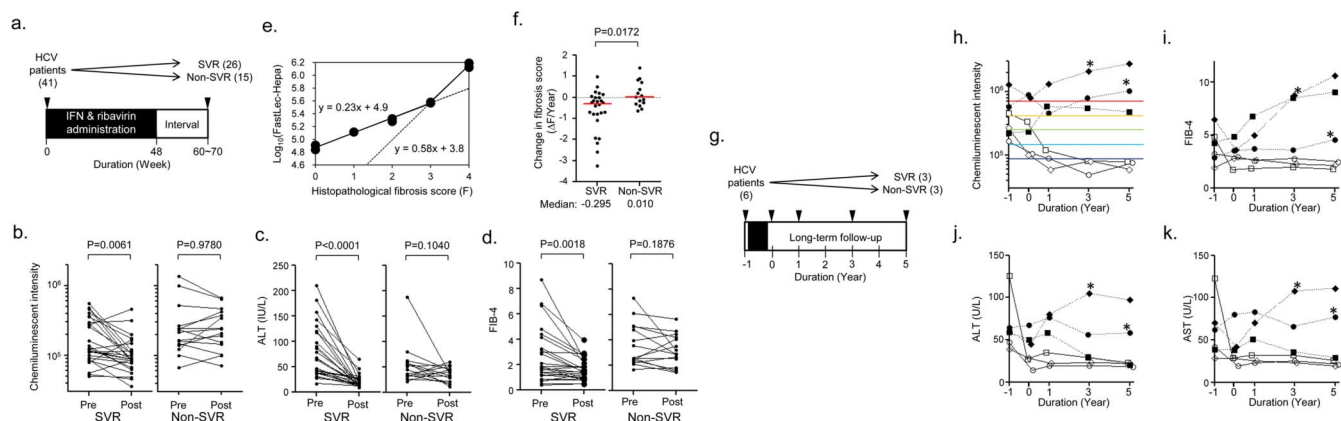

Figure 5 | Evaluation of the curative effect of interferon therapy by FastLec-Hepa. (a) Validation of FastLec-Hepa in short-interval evaluation. The numbers in parentheses represent the number of patients participated in this experiment. Arrowheads indicate the timing of blood collection. At week 0, blood was collected immediately before the treatment. Black box indicates the period of PEG-interferon-α and ribavirin therapy. Changes in the FastLec-Hepa counts (b), ALT (c), and the FIB-4 index (d) in patients with sustained virologic response (SVR) and relapse/nonresponders (non-SVR) during interferon therapy. The *P*-value was determined by a nonparametric method, the Wilcoxon matched pairs signed-rank test. (e) Dot-plot representation of the histopathological fibrosis score and the medians of FastLec-Hepa counts. Best-fit linear curves were calculated in Excel 2007 (Microsoft) allowing conversion of the FastLec-Hepa counts into fibrosis score. (f) Yearly changes in the converted fibrosis score. Changes for patients with SVR and non-SVR are indicated in the dot plots. Red horizontal lines represent the median. The *P*-value was determined by the Mann–Whitney *U* test. (g) Validation of FastLec-Hepa in long-term follow-up. The numbers in parentheses represent the number of patients participated in this experiment. Arrowheads indicate the timing of blood collection. At year -1 and 0, the blood was collected immediately before and after the treatment, respectively. Black box indicates the period of PEG-interferon-α and ribavirin therapy. Yearly changes of FastLec-Hepa counts (h), FIB-4 index (i), ALT (j), and AST (k) in individual patients after therapy. The five colored lines in (h) represent the median values obtained for each fibrosis stage (red, F4; orange, F3; green, F2; cyan, F1; blue, F0). Closed and opened symbols indicate the data obtained from non-SVR and SVR patients, respectively. * indicates the period when the development of HCC was found.

particularly for revealing and managing patients at a high risk of progression to liver complications such as HCC and related life-threatening events. The most striking advantage of FastLec-Hepa is not only its simplicity but also its capacity to provide fibrosis read-outs that are not influenced by fluctuations in the ALT value or inflammation, both of which can cause falsely high estimates in most of the other fibrosis tests available[10]. In fact, our study has illustrated robust capacity of FastLec-Hepa to evaluate the effects of antiviral therapy and subsequent disease progression in both the short and long term.

Many retrospective and prospective studies have demonstrated that achieving SVR through the PEG-interferon-α/ribavirin treatment significantly reduces liver-related morbidity and mortality (i.e., hepatic decompensation, HCC, and liver-related death)[28–30]. As this combination therapy is effective in only about 50% of patients with HCV genotype 1, new agents[1] and targets[31] for antiviral treatments of HCV have been developed to achieve SVR more effectively after the therapy. Long-term follow-ups often show that the risk of disease progression is significantly high in patients with non-SVR after PEG-interferon-α/ribavirin treatment. Furthermore, the development of HCC in patients with SVR remains at a significant cumulative rate (2%)[28,30,32,33]. For these reasons, a new data-mining model using individual factors (age, platelet count, serum albumin and AST) was developed recently to identify patients at a high risk of HCC development[34]. This is, however, a statistical procedure for estimating the chance of disease progression, and there is not a direct evaluation of fibrosis. In the present report, we performed a long-term retrospective study with serially collected sera from SVR and non-SVR patients, in which we showed the potential use of FastLec-Hepa for improved prognostic accuracy. Indeed, recent advances in the development of antifibrotic agents lead us to expect the therapeutic elimination of health risks associated with HCC and decompensation[35]. Moreover, we expect that FastLec-Hepa will be proved for its usefulness in rapid evaluation of progression and regression of fibrosis in clinical trials of newly developed antifibrotic agents. Hence, FastLec-Hepa should be very useful for fibrosis stage screening and evaluation of disease progression in untreated individuals or patients under or after treatment, as well as evaluation of the most recently developed drugs.

It is important to note that FastLec-Hepa has many merits, including speed (possibly 1,000 assays per day) and full automation for measurement of a serological glycobiomarker: these attributes will enable retrospective studies with valuable serum specimens that have been collected previously. In addition, our recently developed calibrator for FastLec-Hepa will improve traceability and enable simultaneous assay and data storage in multiple diagnostic facilities. The data obtained with diluted serum samples demonstrated a high level of assay reproducibility and a very favorable linear detection range (**Supplementary Fig. 14**). Furthermore, we found an excellent agreement between assay values for serum and plasma prepared simultaneously from the same patient. Presently, we have about 10,000 sera and plasma available with detailed clinical notes collected in more than 10 facilities in Japan, and a series of retrospective studies is under way. We will shortly conclude licensing of our system for clinical implementation, based largely on the trials of the present study. In contrast to this, the majority of recent noninvasive techniques are currently shifting to physical measurements such as FibroScan, acoustic radiation force impulse[36] and real-time strain elastography[37]. Any on-site assay of large numbers of blood samples should provide a diagnostic value comparable to that of FibroTest, and a direct comparison in the same patient group will be necessary to evaluate this. We note here that according to a recent statistical validation method[38], predicted AUC of the diagnostic value of FibroTest for detection of advanced fibrosis in our sample set (DANA score = 1.81) was approximately 0.77, which was comparable to the AUC of FastLec-Hepa we obtained (0.79).

FastLec-Hepa has adopted a new paradigm for clinical diagnosis, "glyco-diagnosis", which is based on the quantity and quality of protein glycosylation patterns that well indicate disease progression. To detect such changes in glycosylation by conventional methods (e.g., mass spectrometry, liquid chromatography, or capillary electrophoresis), it is absolutely necessary to liberate the glycans of interest from their protein linkages[15,17,39]. It is possible to employ an alternative technology, which is based on a lectin–antibody sandwich immunodetection system for intact glycoproteins bearing disease-specific glyco-alterations. Such assays have been used to detect changes in fucosylation of *N*-linked glycans, which are associated with liver disease. However, in the present study, fucose-binding lectins were classified as "high noise" (**Fig. 2b**), and thus an enrichment of the target protein was the essential process in the assay. Lectin-overlay detection is performed typically after on-plate enrichment of the target glycoproteins by an immobilized antibody. In such cases, detection relies on a low avidity (high dissociation rate) between the captured glycoprotein and the overlaid lectin probe (see *right* of **Supplementary Fig. 3b**). These kinetic considerations essentially eliminate the use of an automated bedside clinical chemistry analyzer. Even though a fucose-binding lectin was immobilized on the beads (see *left* of **Supplementary Fig. 3b**), it still remains a problem for reliable quantitation by autoanalyzer. Our previous system LecT-Hepa[16,18,19,26], which detects the level of fucosylated α1-acid glycoprotein, requires enrichment of the protein prior to the assay.

In the present study, we have developed a strategy to overcome these problems in glyco-diagnosis associated with clinical implementation, and realized a rapid "on-site diagnosis" system (17 min, within the minimum time required for single assay by HISCL), based on analysis of a glycomarker (**Supplementary Fig. 1**). The strategy for selecting the most robust lectin led us to WFA, and away from the use of fucose-binding lectins, for the direct measurement system (**Fig. 2**). The diagnostic utility of M2BP, a protein resembling "sweet-doughnut"[20], brought a favorable density and orientation of the disease-related glycan on the homomultimer. These characteristic structures resulted in a major increase in the avidity of M2BP for the plated WFA. The resulting glycan–lectin interaction, which is remarkably strong and specific, made it possible to develop the rapid and highly sensitive assay (see *left* of **Supplementary Fig. 3b**). We believe that this unique strategy will revolutionize the use of glyco-diagnosis in clinical medicine and potentially provide a framework for the development of a new generation of biomarker assays.

Methods

Patient samples, biochemical parameters and indices. Patients with chronic hepatitis were enrolled at Nagoya City University Hospital and Hokkaido University Hospital. Healthy volunteers as the controls were randomly selected in Nagoya City University Hospital (70 individuals) and AIST (48 individuals). The institutional ethics committees at Nagoya City University Hospital, Hokkaido University Hospital, and AIST approved this study, and informed consent for the use of their clinical specimens was obtained from all participants before the collection. In addition, we used 1,000 serum samples from virus-negative Caucasians as the normal population, which were purchased from Complex Antibodies Inc. (Fort Lauderdale, FL) and collected under IRB-approved collection protocols. Fibrosis was graded in the patients according to the histological activity index (HAI) using biopsy or surgical specimens. Biopsy specimens were classified as follows: F0, no fibrosis; F1, portal fibrosis without septa; F2, few septa; F3, numerous septa without cirrhosis; and F4, cirrhosis. The three diagnostic targets in this study were defined as significant fibrosis: F2+F3+F4; severe fibrosis: F3+F4; and cirrhosis: F4. Hepatic inflammation was also assessed according to the HAI, as follows: A0, no activity; A1, mild activity; A2, moderate activity; and A3, severe activity. Cirrhosis was confirmed by ultrasonography (coarse liver architecture, nodular liver surface, and blunt liver edges), evidence of hypersplenism (splenomegaly on ultrasonography) and/or a platelet count of < 100,000/mm³. Virological responses during PEG-interferon-α and ribavirin therapy were defined as follows[5]: SVR, absence of HCV RNA from serum 24 weeks following discontinuation of therapy; nonresponder, failure to clear HCV RNA from serum after 24 weeks of therapy; relapse, reappearance of HCV RNA in serum after therapy was discontinued. For all patients, age and sex were recorded and serum levels of the following were analyzed: aspartate aminotransferase (AST), alanine aminotransferase (ALT), γ-glutamyltransferase (GGT), total bilirubin,

albumin, cholinesterase, total cholesterol, platelet count (PLT), hyaluronic acid (HA). The FIB-4 index was calculated as follows: [age (years) $\times$ AST (U/L)]/[platelets $(10^9/L) \times$ ALT $(U/L)^{1/2}]^{26}$. Fibrosis-specific glyco-alteration of α1-acid glycoprotein was determined by lectin–antibody sandwich immunoassays with a combination of three lectins (*Datura stramonium* agglutinin (DSA), *Maackia amurensis* leukoagglutinin (MAL), and *Aspergillus oryzae* lectin (AOL))[16]. All assays used an automated chemiluminescence enzyme immunoassay system (HISCL-2000i; Sysmex Co., Kobe, Japan)[18].

Enrichment of M2BP from serum. An automated protein purification system (ED-01; GP BioSciences Ltd., Yokohama, Japan) was used to immunoprecipitate M2BP from serum specimens. In brief, sera (2 μl) were diluted 10-fold with PBS/0.2%(w/v) SDS, heated at 95°C for 20 min, mixed with 10 μl of Triton X-100 in TBS (TBSTx) and injected into a 96-well SUMILON microtiter plate (Sumitomo Bakelite Co., Ltd., Tokyo, Japan). The plate and working reagents, including biotinylated anti-M2BP antibody (10 ng/μl), streptavidin-coated magnetic beads, washing buffer (1% TBSTx) and elution buffer (TBS containing 0.2% SDS), were loaded into the system. This generated 110 μl of purified M2BPs per serum sample (96 samples in 3.5 h).

Western blot analysis. Anti-human M2BP polyclonal antibody was purchased from R&D Systems, Inc. (Minneapolis, MN) and biotinylated with Biotin Labeling Kit – NH$_2$ (Dojindo Laboratories, Kumamoto, Japan). Purified serum M2BPs were electrophoresed under reducing conditions on 5–20% polyacrylamide gels (DRC, Tokyo, Japan) and transferred to PVDF membranes. After treatment with Block Ace® (DS Pharma Biomedical Co., Ltd., Osaka, Japan), the membranes were incubated with biotinylated anti-M2BP polyclonal antibody, and then with alkaline phosphatase-conjugated streptavidin (1/5000 diluted with TBST; ProZyme, Inc., San Leandro, CA). The membranes were incubated with Western Blue stabilized substrate for alkaline phosphatase (Promega, Madison, WI).

Lectin microarray analysis. Enriched M2BPs were analyzed with an antibody-overlay lectin microarray[24]. Purified protein (14 μl) was diluted to 60 μl with PBS containing 1%(v/v) Triton X-100 (PBSTx); this was applied to a LecChip™ (GP BioSciences Ltd.), which included three spots of 45 lectins in each of seven reaction wells. After incubation for 12 h at 20°C, 2 μl of human serum IgG (10 mg/ml) was added to the reaction solution on each chip and incubated for 30 min. The reaction solution was then discarded, and the chip was washed three times with PBSTx. Subsequently, 60 μl (200 ng) of biotinylated anti-human M2BP in PBSTx was applied to the chip, and incubated for 1 h. After three washes with PBSTx, 60 μl (400 ng) of a Cy3-labeled streptavidin (GE Healthcare, Buckinghamshire, UK) solution in PBSTx was added and incubated for 30 min. The chip was rinsed with PBSTx, scanned with an evanescent-field fluorescence scanner (GlycoStation™ Reader1200; GP BioSciences Ltd.) and analyzed with the Array Pro Analyzer software package, version 4.5 (Media Cybernetics, Inc., Bethesda, MD). The chip was scanned with the gain set to register a maximum net intensity < 40,000 for the most intense spots. The net intensity value for each spot was calculated by subtracting the background value from the signal intensity value. The relative intensity of lectin-positive samples was determined from the ratio of their fluorescence to the fluorescence of the internal-standard lectin, DSA.

Quantitation of *Wisteria floribunda* agglutinin (WFA)-binding M2BP. Serum was pretreated as described above under enrichment of M2BP from serum. Pretreated samples (50 μl) were diluted with an equal volume of starting buffer (0.1%(w/v) SDS in PBSTx), added to the WFA-coated agarose in a microtube (20 μl slurry; Vector Lab., Burlingame, UK), and incubated at 4°C for 5 h with gentle shaking. After centrifugation of the reaction solution at 2000 $\times$ g for 10 min, the supernatant was removed to a new microtube. The precipitate was suspended in 50 μl of the starting buffer, recentrifuged and this second supernatant combined with the first (designated as path-through fraction T). The precipitate was then washed with 200 μl of the starting buffer and the bound glycoproteins were eluted with 60 μl of 200 mM galactosamine/0.02%(w/v) SDS in PBS (designated as elution fraction E). M2BP was immunoprecipitated from fractions T and E and examined by electrophoresis under reducing conditions on 5–20% gradient SDS–polyacrylamide gels.

WFA-antibody sandwich ELISA. Flat-bottomed 96-well streptavidin-precoated microtiter plates (Nunc, Int., Tokyo, Japan) were treated with biotinylated WFA (Vector, 250 ng/well) for 1 h at room temperature. The plates were incubated with the diluted serum samples (50 μl) in PBS containing 0.1%(v/v) Tween20 (PBS-t) for 2 h at room temperature and then with 50 ng/well of the anti-human M2BP polyclonal antibody, in PBS-t for 2 h at room temperature. The plates were washed extensively and then incubated with 50 μl of horseradish peroxidase (HRP)-conjugated anti-mouse IgG (Jackson ImmunoResearch Laboratories Inc., Philadelphia, PA) at 1:10,000 in PBS-t for 1 h at room temperature. The substrate 3,3',5,5'-tetramethylbenzidine (Thermo Fisher Scientific, Fremont, CA) solution (100 μl) was added to each well. The enzyme reaction was stopped by adding 100 μl of 1 M sulfuric acid, and the optical density measured at 450 nm.

WFA-antibody sandwich immunoassay by HISCL. The fibrosis-specific form of glycosylated M2BP was measured based on a sandwich immunoassay approach. Glycosylated M2BP was captured by WFA immobilized on magnetic beads, and the bound product was assayed with an anti-human M2BP monoclonal antibody linked to alkaline phosphatase (ALP-αM2BP). Two reagent packs (M2BP-WFA detection

pack and a chemiluminescence substrate pack) were loaded in the HISCL. The detection pack comprised three reagents: a reaction buffer solution (R1), a WFA-coated magnetic beads solution (R2) and an ALP-αM2BP solution (R3). The chemiluminescence substrate reagent pack contained a CDP-Star substrate solution (R4) and a stopping solution (R5). Typically, serum (10 μl) was diluted to 60 μl with R1 and then mixed with R2 (30 μl). After the binding reaction, R3 (100 μl) was added to the reaction solution. The resultant conjugates were magnetically separated from unbound components, and mixed well with R4 (50 μl) and R5 (100 μl) before reading of the fluorescence. The chemiluminescent intensity was acquired within a period of 17 min in the operation described above. The reaction chamber was kept at 42°C throughout.

Statistics. Statistical analyses and graph preparation used Dr. SPSS II Windows software (SPSS Co., Tokyo, Japan), GraphPad Prism 5.0 (GraphPad Software Inc., La Jolla, CA), and Windows Excel 2007. This facilitated selection of the optimal lectin for analysis of fibrosis and a comparison of the diagnostic value of other serological fibrosis markers and indices. Because the data distribution for each parameter was non-Gaussian, the *P*-values were determined by nonparametric tests, such as the Mann–Whitney *U* test and Wilcoxon signed-rank test. Correlations with liver fibrosis were estimated as the significance of differences among the staging groups (F0–1, F2, F3, and F4) determined by Kruskal–Wallis nonparametric one-way analysis of variance. To assess classification efficiencies for detecting significant fibrosis, severe fibrosis and cirrhosis, the receiver-operating characteristic (ROC) curve analysis was also carried out to determine the area under the curve (AUC) values. Cutoff values obtained from Youden's index were used to classify patients. Diagnostic accuracy was expressed in terms of specificity, sensitivity and AUC.

1. "Nature Outlook Hepatitis C" edited by Brody, H. *et al. Nature* **474**, S1–S21 (2011).
2. Ge, D. *et al.* Genetic variation in IL28B predicts hepatitis C treatment-induced viral clearance. *Nature* **461**, 399–401 (2009).
3. Suppiah, V. *et al.* IL28B is associated with response to chronic hepatitis C interferon-alpha and ribavirin therapy. *Nat. Genet.* **41**, 1100–1104 (2009).
4. Tanaka, Y. *et al.* Genome-wide association of IL28B with response to pegylated interferon-alpha and ribavirin therapy for chronic hepatitis C. *Nat. Genet.* **41**, 1105–1109 (2009).
5. Ghany, M. G., Strader, D. B., Thomas, D. L. & Seeff, L. B. Diagnosis, management, and treatment of hepatitis C: an update. *Hepatology* **49**, 1335–1374 (2009).
6. Afdhal, N. H. *et al.* hepatitis C pharmacogenetics: state of the art in 2010. *Hepatology* **53**, 336–345 (2011).
7. Peng, C. Y., Chien R. N. & Liaw, Y. N. Hepatitis B virus-related decompensated liver cirrhosis: benefits of antiviral therapy. *J. Hepatol.* **57**, 442–450 (2012).
8. Chang, T. T. *et al.* Long-term entecavir therapy results in the reversal of fibrosis/cirrhosis and continued histological improvement in patients with chronic hepatitis B. *Hepatology* **52**, 886–893 (2010).
9. Shiratori, Y. *et al.* Histologic improvement of fibrosis in patients with hepatitis C who have sustained response to interferon therapy. *Ann. Intern. Med.* **132**, 517–524 (2000).
10. Castera, L. Non-invasive assessment of liver fibrosis in chronic hepatitis C. *Hepatol. Int.* **5**, 625–634 (2011).
11. Imbert-Bismut, F. *et al.* Biochemical markers of liver fibrosis in patients with hepatitis C virus infection: a prospective study. *Lancet* **357**, 1069–1075 (2001).
12. Calès, P. *et al.* A novel panel of blood markers to assess the degree of liver fibrosis. *Hepatology* **42**, 1373–1381 (2005).
13. Castera, L. *et al.* Prospective comparison of two algorithms combining non-invasive methods for staging liver fibrosis. *J. Hepatol.* **52**, 191–198 (2010).
14. Boursier, J. *et al.* Comparison of eight diagnostic algorithm for liver fibrosis in hepatitis C: new algorithms are more precise and entirely noninvasive. *Hepatology* **55**, 58–67 (2012).
15. Callewaert, N. *et al.* Noninvasive diagnosis of liver cirrhosis using DNA sequencer-based total serum protein glycomics. *Nat. Med.* **10**, 429–434 (2004).
16. Kuno, A. *et al.* Multilectin assay for detecting fibrosis-specific glyco-alteration by means of lectin microarray. *Clin. Chem.* **57**, 48–56 (2011).
17. Vanderschaeghe, D. *et al.* High-throughput profiling of the serum N-glycome on capillary electrophoresis microfluidics systems: toward clinical implementation of GlycoHepatoTest. *Anal. Chem.* **82**, 7408–7415 (2010).
18. Kuno, A. *et al.* LecT-Hepa: A triplex lectin-antibody sandwich immunoassay for estimating the progression dynamics of liver fibrosis assisted by a bedside clinical chemistry analyzer and an automated pretreatment machine. *Clin. Chim. Acta* **412**, 1767–1772 (2011).
19. Du, D. *et al.* Comparison of LecT-Hepa and FibroScan for assessment of liver fibrosis in hepatitis B virus infected patients with different ALT levels. *Clin. Chim. Acta* **413**, 1796–1799 (2012).
20. Sasaki, T., Brakebusch, C., Engel, J. & Timpl, R. Mac-2 binding protein is a cell-adhesive protein of the extracellular matrix which self-assembles into ring-like structures and binds beta1 integrins, collagens and fibronectin. *EMBO J.* **17**, 1606–1613 (1998).
21. Iacovazzi, P. A. *et al.* Serum 90K/MAC-2BP glycoprotein in patients with liver cirrhosis and hepatocellular carcinoma: a comparison with alpha-fetoprotein. *Clin. Chem. Lab. Med.* **39**, 961–965 (2001).

22. Artini, M. *et al*. Elevated serum levels of 90K/MAC-2 BP predict unresponsiveness to alpha-interferon therapy in chronic HCV hepatitis patients. *J. Hepatol.* **25**, 212–217 (1996).

23. Cheung, K. J. *et al*. The HCV serum proteome: a search for fibrosis protein markers. *J. Viral. Hepat.* **16**, 418–429 (2009).

24. Kuno, A. *et al*. Focused differential glycan analysis with the platform antibody-assisted lectin profiling for glycan-related biomarker verification. *Mol. Cell. Proteomics* **8**, 99–108 (2008).

25. Kuno, A. *et al*. Evanescent-field fluorescence-assisted lectin microarray: a new strategy for glycan profiling. *Nat. Met.* **2**, 851–856 (2005).

26. Vallet-Pichard, A. *et al*. FIB-4: an inexpensive and accurate marker of fibrosis in HCV infection. Comparison with liver biopsy and fibrotest. *Hepatology* **46**, 32–36 (2007).

27. Ito, K. *et al*. LecT-Hepa, a glyco-marker derived from multiple lectins, as a predictor of liver fibrosis in chronic hepatitis C patients. *Hepatology* **56**, 1448–1456 (2012).

28. Bruno, S. *et al*. Sustained virological response to interferon-α is associated with improved outcome in HCV-related cirrhosis: A retrospective study. *Hepatology* **45**, 579–587 (2007).

29. Cardoso, A.-C. *et al*. Impact of peginterferon and ribavirin therapy on hepatocellular carcinoma: Incidence and survival in hepatitis C patients with advanced fibrosis. *J. Hepatol.* **52**, 652–657 (2010).

30. Morgan, T. R. *et al*. Outcome of sustained virological responders with histologically advanced chronic hepatitis C. *Hepatology* **52**, 833–844 (2010).

31. Lupberger, J. *et al*. EGFR and EphA2 are host factors for hepatitis C virus entry and possible targets for antiviral therapy. *Nat. Med.* **17**, 589–595 (2011).

32. Iwasaki, Y. *et al*. Risk factors for hepatocellular carcinoma in hepatitis C patients with sustained virologic response to interferon therapy. *Liver Int.* **24**, 603–610 (2004).

33. Ikeda, K. *et al*. Anticarcinogenic impact of interferon on patients with chronic hepatitis C: A large-scale long-term study in a single center. *Intervirology* **49**, 82–90 (2006).

34. Kurosaki, M. *et al*. Data mining model using simple and readily available factors could identify patients at high risk for hepatocellular carcinoma in chronic hepatitis C. *J. Hepatol.* **56**, 602–608 (2012).

35. Schuppan, D. & Pinzani, M. Anti-fibrotic therapy: lost in translation? *J. Hepatolol.* **56**, S66–74 (2012).

36. Rizzo, L. *et al*. Comparison of transient elastography and acoustic radiation force impulse for non-invasive staging of liver fibrosis in patients with chronic hepatitis C. *Am. J. Gastroenterol.* **106**, 2112-2120 (2011).

37. Ferraioli, G. *et al*. Performance of real-time sitrain elastography, transient elastgraphy, and aspartate-to-platelet ration index in the assessment of fibrosis in chronic hepatitis C. *AJR Am. J. Roentgenol.* **199**, 19–25 (2012).

38. Poynard, T. *et al*. Standardization of ROC curve areas for diagnostic evaluation of liver fibrosis markers based on prevalences of fibrosis stages. *Clin. Chem.* **53**, 1615–1622 (2007).

39. Nishimura, S. Toward automated glycan analysis. *Adv. Carbohydr. Chem. Biochem.* **65**, 219–271 (2011).

Acknowledgments

Author contributions:

A.K. conceived and designed the study, performed most of the biochemical experiments, analyzed data and wrote the paper with comments from Y.T., M.M. and H.N.; Y.I. conceived and designed the study, performed the sample pre-treatment for the assay, and analyzed data; Y.T., K.I., M.M., and S.H collected clinical samples, designed the validation study, and analyzed data; A.M. and S.S. performed the biochemical experiments including lectin microarray analysis and analyzed data; M.S. and M.K. performed staging of biopsy specimens by histological activity index (HAI); H.N. conceived and designed the study, and supervised all aspects of the work; and all authors discussed the results and implications, and commented on the paper.

Additional information

How to cite this article: Kuno, A. *et al*. A serum "sweet-doughnut" protein facilitates fibrosis evaluation and therapy assessment in patients with viral hepatitis. *Sci. Rep.* **3**, 1065; DOI:10.1038/srep01065 (2013).